Structure of Spa15, a type III secretion chaperone from Shigella flexneri with broad specificity

Eerde, André van; Hamiaux, Cyril; Pérez, Javier; Parsot, Claude; Dijkstra, Bauke W.

Published in:
Default journal

DOI:
10.1038/sj.embor.7400144

Publication date:
2004

EMBO reports

scientific report

Structure of Spa15, a type III secretion chaperone from *Shigella flexneri* with broad specificity

André van Eerde[1], Cyril Hamiaux[1], Javier Pérez[2], Claude Parsot[3] & Bauke W. Dijkstra[1+]

[1]Laboratory of Biophysical Chemistry, University of Groningen, Groningen, The Netherlands, [2]LURE, Centre Universitaire Paris-Sud, Orsay, France, and [3]Unité de Pathogénie Microbienne Moléculaire INSERM U389, Institut Pasteur, Paris, France

Type III secretion (TTS) systems are used by many Gram-negative pathogens to inject virulence proteins into the cells of their hosts. Several of these virulence effectors require TTS chaperones that maintain them in a secretion-competent state. Whereas most chaperones bind only one effector, Spa15 from the human pathogen *Shigella flexneri* and homologous chaperones bind several seemingly unrelated effectors, and were proposed to form a special subgroup. Its 1.8 Å crystal structure confirms this specific classification, showing that Spa15 has the same fold as other TTS effector chaperones, but forms a different dimer. The presence of hydrophobic sites on the Spa15 surface suggests that the different Spa15 effectors all possess similar structural elements that can bind these sites. Furthermore, the Spa15 structure reveals larger structural differences between class I chaperones than previously anticipated, which does not support the hypothesis that chaperone–effector complexes are structurally conserved and function as three-dimensional secretion signals.

Keywords: type III secretion; Spa15; chaperone; *Shigella*; crystal structure

EMBO reports (2004) **5**, 477–483. doi:10.1038/sj.embor.7400144

INTRODUCTION

The type III secretion (TTS) pathway is used by numerous Gram-negative bacteria that are pathogenic for humans, animals and plants to deliver proteins within or beyond the membrane of cells of their hosts. TTS systems consist of (i) a TTS apparatus (TTSA) that spans the bacterial envelope and protrudes from the bacterial surface, (ii) two translocators that transit through the TTSA and insert into the cell membrane to form a pore, (iii) effectors that transit through the TTSA and the translocation pore, and are injected into cells where they interfere with cellular processes, and (iv) specific chaperones that associate in the bacterial cytoplasm with translocators and some effectors before the transit of these proteins through the TTSA (Hueck, 1998). The nature of the signal that addresses effectors and translocators to the TTSA is still controversial (Cornelis, 2003; Ramamurthi & Schneewind, 2003). However, there is strong evidence for the presence of a secretion signal within the first 15 residues of stored proteins. Before their transit through the TTSA, effectors and translocators need to be stabilized and maintained in a secretion-competent state in the bacterial cytoplasm. Specialized, energy-independent chaperones, designated TTS chaperones, participate in these functions, although their exact role is still poorly understood (Parsot *et al*, 2003).

All TTS chaperones have a small size and acidic pI, but not all TTS chaperones exhibit sequence similarities. TTS chaperones have been divided into two general groups: class I is specific for effector proteins, whereas class II assists translocator proteins. Class I was further divided into two subclasses on the basis of the number of substrates (one for class IA versus several for class IB) and the respective location of the genes encoding the chaperone and its substrate(s) (adjacent for class IA versus dispersed for class IB) (Parsot *et al*, 2003). The three-dimensional (3D) structures of class IA chaperones, including those of SicP and SigE from *Salmonella enterica*, SycE from *Yersinia pseudotuberculosis* and CesT from enteropathogenic *Escherichia coli* (EPEC), exhibit striking similarities despite the low sequence similarity shared by these proteins (Birtalan & Ghosh, 2001; Luo *et al*, 2001; Stebbins & Galán, 2001; Evdokimov *et al*, 2002). They have similar folds, consisting of a twisted β-sheet with three α-helices packed against it, and form very similar dimers. The details of the effector binding are revealed by the structures of complexes between SycE and YopE(23–78) (Birtalan *et al*, 2002) and SicP and SptP(36–139) (Stebbins & Galán, 2001). In both cases, the binding region of the effector is wrapped around the surface of the chaperone dimer as an extended polypeptide. The structural similarity of these two complexes has led to the proposal that class I chaperone–effector complexes might constitute a general 3D secretion signal recognized by the TTSA (Birtalan *et al*, 2002).

The TTS system of *Shigella flexneri*, a bacterium that causes bacillary dysentery in humans, contains the chaperone Spa15 that has been the basis for distinguishing the subclass IB chaperones (Page *et al*, 2002; Parsot *et al*, 2003). Spa15 exhibits an extended binding specificity, as it chaperones the effectors IpaA, IpgB1,

[1]Laboratory of Biophysical Chemistry, University of Groningen, Nijenborgh 4, 9747 AG Groningen, The Netherlands
[2]LURE, Centre Universitaire Paris-Sud, 91898 Orsay Cedex, France
[3]Unité de Pathogénie Microbienne Moléculaire INSERM U389, Institut Pasteur, 75724 Paris Cedex 15, France
[+]Corresponding author. Tel: +31 503634381; Fax: +31 503634800;
E-mail: bauke@chem.rug.nl

Received 5 January 2004; revised 5 March 2004; accepted 12 March 2004; published online 16 April 2004

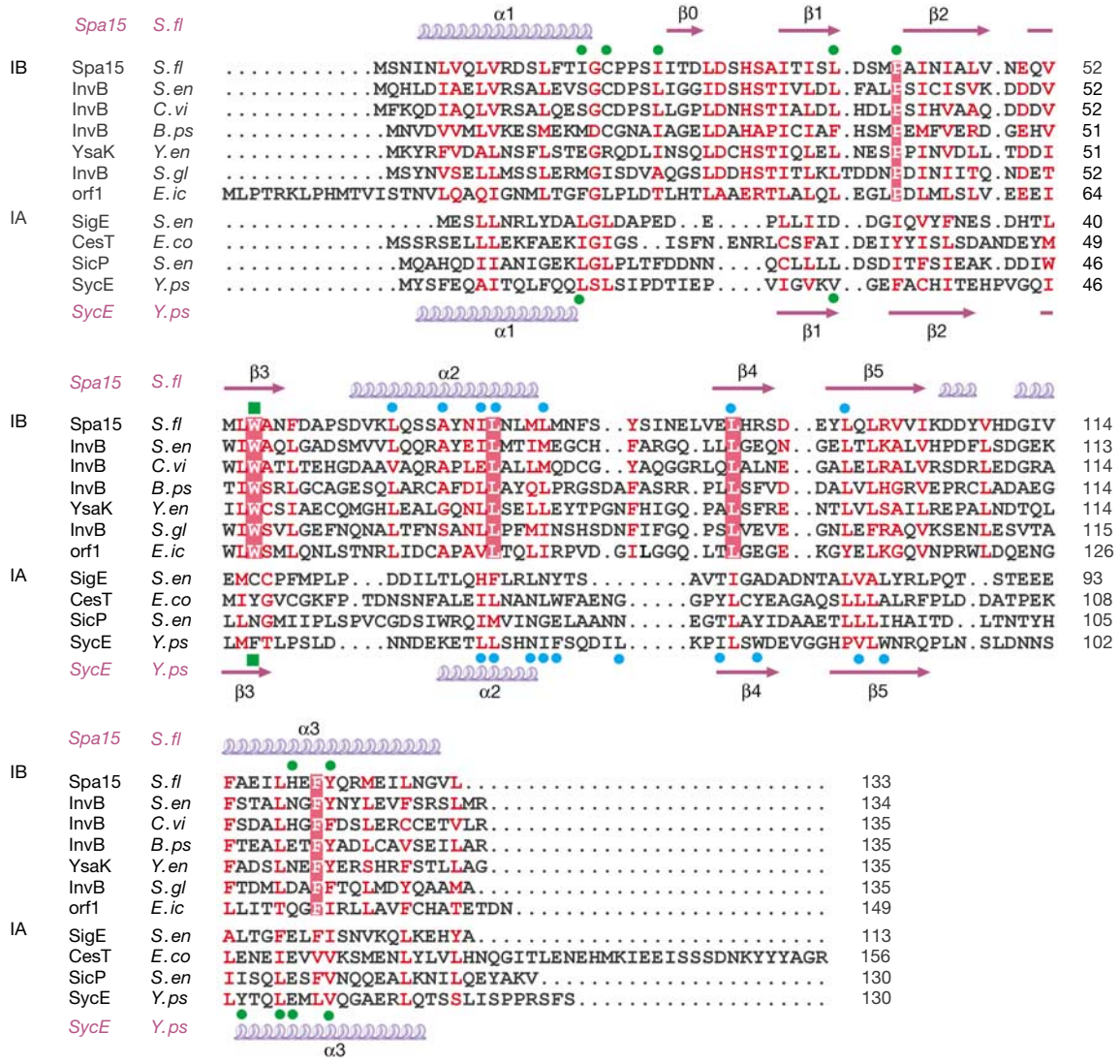

Fig 1 | Sequence alignment of class I TTS chaperone family members. Sequences of putative class IB chaperones are aligned with Spa15. Alignment of class IA sequences to Spa15 is structure-based. Secondary structure of Spa15 and of SycE is indicated above and below the sequences, respectively. Conserved residues are in red, with absolutely conserved residues shaded red. Indicated above and below the sequences for Spa15 and SycE, respectively, are residues forming the hydrophobic pocket (green dots), helix-binding groove (green square) and dimer contacts (blue dots). Sequences are *S. flexneri* Spa15 (CAC05823), *S. enterica* InvB (AAA74037), *Chromobacterium violaceum* InvB (AAQ60299), *Burkholderia pseudomallei* InvB (*B. pseudomallei* unfinished genome, http://www.tigr.org), *Yersinia enterocolitica* YsaK (AAK84111), *Sodalis glossinidius* InvB (AAG48601), *Edwardsiella ictaluri* Orf1 (AAF85960), *S. enterica* SigE (CAD08216), enteropathogenic *E. coli* CesT (AAL57550), *S. enterica* SicP (AAL21759) and *Y. pseudotuberculosis* SycE (AAK69248).

OspC3 and probably also OspB (Page *et al*, 2001, 2002). These effectors have different molecular sizes and do not share any detectable sequence similarity. Recently, the *S. enterica* homologue of Spa15, InvB, has also been reported to be the chaperone of at least three effectors (Ehrbar *et al*, 2003). The fact that Spa15 and other class IB chaperones are encoded by genes located within operons for components of the TTSA and that these chaperones have several substrates has led to the proposal that class IB chaperones might represent an ancient form of TTS chaperones (Parsot *et al*, 2003). However, in the absence of sequence similarities between class IB and class IA chaperones (Fig 1), the structural relationship between the two classes of chaperones and the potential mode of binding of class IB chaperones were not known. Here, we have determined the X-ray structure of Spa15 and have conducted small-angle X-ray scattering (SAXS) experiments. We show that the class IB chaperone Spa15 is structurally related to class IA chaperones and that structural differences, mainly at the dimer interface, clearly distinguish it from class IA chaperones. The similarity suggests that class IB chaperones probably bind and stabilize their effectors in the same way as class IA chaperones. In addition, Spa15 shows that the structural differences between class I chaperones are much larger than was previously anticipated, which does not support the recent hypothesis that chaperone–effector complexes could function as a structurally conserved 3D secretion signal in TTS of the effectors.

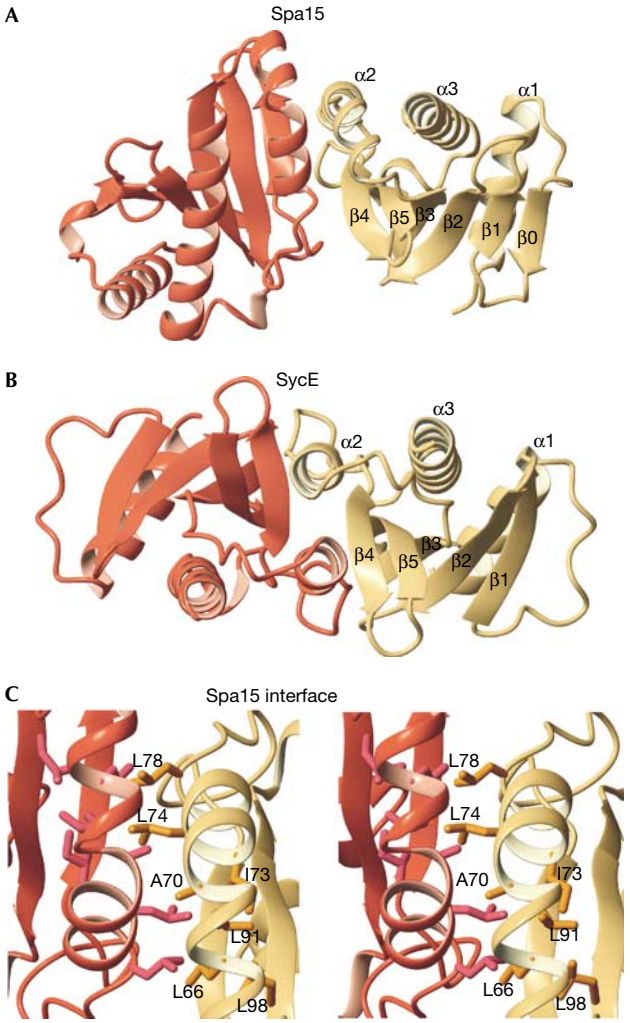

Fig 2 | Subunit organization in class I TTS chaperones. (**A**) Structure of the Spa15 dimer. (**B**) Structure of the SycE dimer (PDB code 1L2W; Birtalan *et al*, 2002). Right-hand chaperone subunits are shown in the same orientation. (**C**) Spa15 dimer interface, viewed perpendicular to the pseudo-twofold axis.

RESULTS

Overall structure and shape

Both space groups in which Spa15 was crystallized show identical intimate associations between two Spa15 molecules. All 133 residues of the native Spa15 could be located in density for each subunit of the dimer, but the 12-residue N-terminal His-tag sequences are disordered. Each subunit consists of a highly twisted six-stranded β-sheet with three α-helices packed against it and exhibits the same overall fold as class IA TTS chaperones (Fig 2) (Birtalan & Ghosh, 2001; Luo *et al*, 2001; Stebbins & Galán, 2001). However, considerable deviations exist between Spa15 and class IA chaperones, as shown by the large root-mean-square deviation of 4.1 Å between 119 Cα atoms of the Spa15 and SycE monomers. Whereas the core secondary structure elements are conserved, substantial variations are present in the loop conformations and the orientation and position of the α2 helix that constitutes the dimer interface.

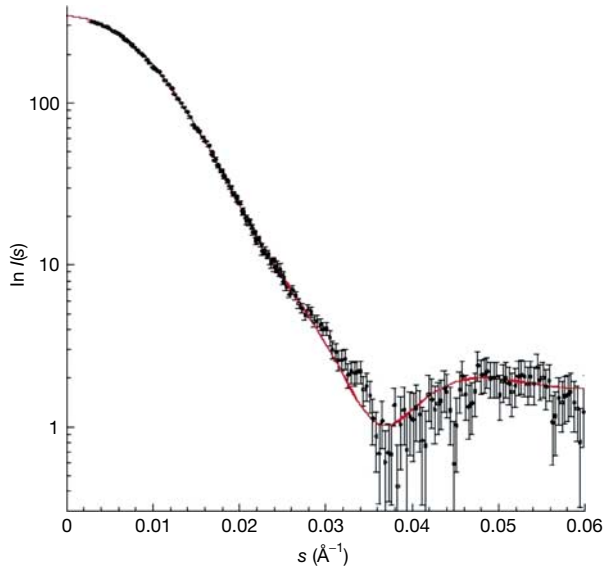

Fig 3 | Comparison between measured SAXS data and the scattering curve calculated from the crystallographic Spa15 dimer.

The most conspicuous difference between Spa15 and class IA chaperones is the relative orientation of the two subunits in the dimer. This is a direct result of the different orientations of the α2 helices of the two subunits that, in Spa15, contact each other under an angle of about 30°. In contrast, the α2 helices of SycE, SigE, CesT and SicP run parallel, making contacts not only with each other but also with the adjacent β-sheet (Fig 2) (Birtalan & Ghosh, 2001; Luo *et al*, 2001; Stebbins & Galán, 2001). In Spa15, a bend in the helix at Ala 70 maximizes the interaction area at the tip of the dimer. Several leucine and isoleucine residues (Leu 66, Ile 73, Leu 74, Leu 78, Leu 91, Leu 98) contribute to the interface, making the interaction surface quite hydrophobic (Fig 2C). The loop at the C-terminal end of α2 is longer than that for class IA chaperones and provides additional contacts. Some 900 Å^2 of the surface of each Spa15 monomer is buried in the interface, which is less than the values found for class IA chaperones, typically between 1,100 and 1,300 Å^2, but still involves about 13% of the total accessible surface area.

To investigate whether the same elongated dimer of Spa15 also occurs in solution, SAXS experiments were conducted. The calculated scattering curve obtained from the crystallographic coordinates of Spa15 is in excellent agreement with the SAXS experimental data (Fig 3), indicating that the dimer in solution has the same elongated and heart-shaped form as that observed in the crystal (Fig 4).

Potential sites for effector binding

A universal binding mode for class I chaperones has been proposed in which secondary structure elements of the effector strongly interact with two different sites on the surface of the chaperone monomer, with each site occurring twice owing to the twofold symmetry of the chaperone dimer (Fig 4) (Birtalan *et al*, 2002; Stebbins & Galán, 2001). The first interaction site is a groove, formed by the exposed face of the twisted β-sheet that, in the complexes of class IA SycE with YopE(23–78) and SicP with SptP(36–139), is occupied by an α-helix of the effector (Fig 5B).

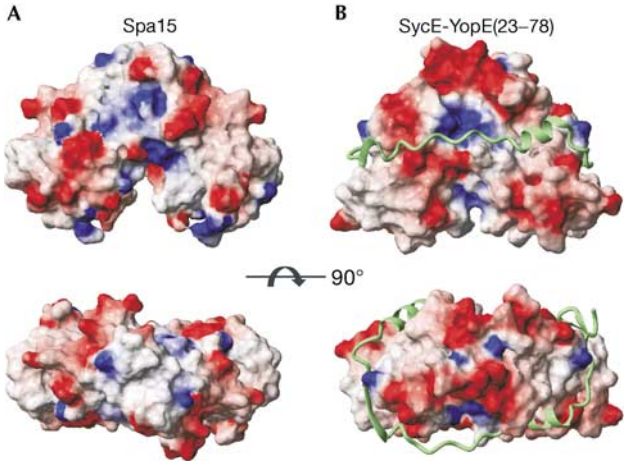

Fig 4 | Comparison of surface and shape between Spa15 and SycE. Orthogonal views of surfaces of (**A**) Spa15 and (**B**) SycE and, in ribbon representation, YopE(23–78). Surfaces coloured according to electrostatic potential.

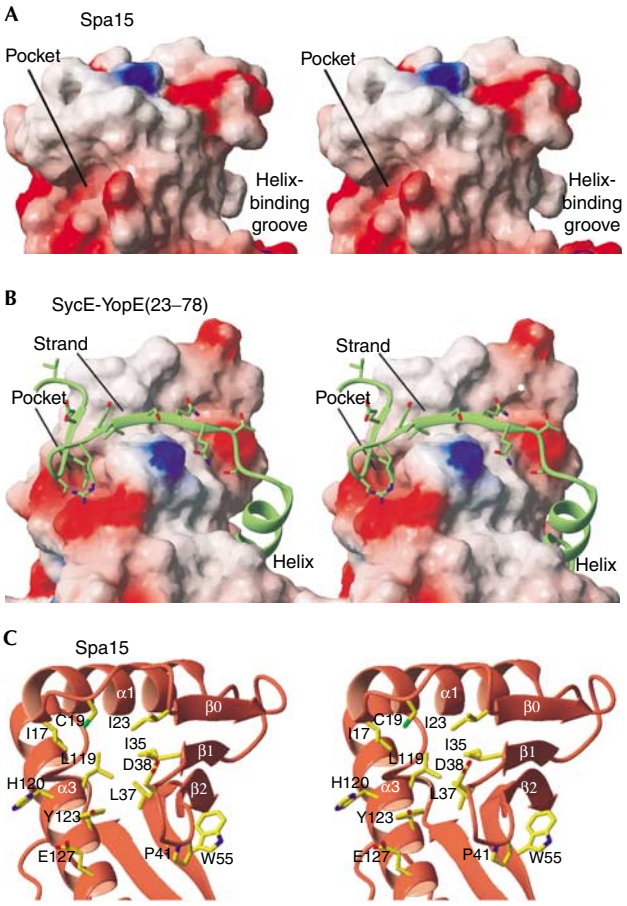

Fig 5 | Hydrophobic interaction sites. (**A**) Spa15 and (**B**) YopE(23–78) bound to SycE. Chaperones in surface representation, coloured according to electrostatic potential. (**C**) Spa15 sites in ribbon representation, orientation identical to (**A**).

Notably, the β-sheet of Spa15 forms a similar groove (Fig 5A) with the bulky Trp 55 occupying a central position. Trp 55 is absolutely conserved among the Spa15 homologues (Fig 1). The conserved location and nature of this groove between class IA and IB chaperones strongly suggest that it might have a helix-binding function in Spa15 as well.

The second interaction site of class IA chaperones is made up of (1) a wedge-shaped shallow groove, formed by strand β1 and the extended loop that connects helix α1 and strand β1, and (2) a deep hydrophobic pocket formed by helix α3, the end of helix α1, and the turn connecting strands β1 and β2. In the class IA chaperone–effector complexes, an extended part of the effector forms an extra β-strand, and hydrophobic side chains occupy the hydrophobic pocket (Fig 5B) (Birtalan *et al*, 2002; Stebbins & Galán, 2001). In contrast, the Spa15 structure does not have such a wedge-shaped groove, although it does have a hydrophobic pocket. The loop connecting α1 and β1, which is distinctly longer in Spa15 and its homologues, has three residues alongside the β-sheet and forms a short extra β-strand, β0 (Figs 2A and 5C). The hydrophobic pocket in Spa15 is at a slightly altered position as compared with the class IA chaperone structures, because helix α1 extends somewhat further and the insertion of Pro 41 changes the backbone conformation of the β1–β2 turn (Fig 5C). Ile 17, Cys 19, Ile 23, Leu 37, His 120 and Tyr 123 are lining the pocket and give it its hydrophobic character. As in class IA chaperones, acidic residues (Asp 38, Glu 127) are present at the far side of this pocket, but the bulky side chain of Tyr 123 restricts the access to the acidic residues by making the pocket distinctly narrower. Taken together, these results suggest that, as described for class IA chaperones, a hydrophobic pocket is an important site of interaction of Spa15 with its effectors.

DISCUSSION

The role of chaperones is central to the function of the TTS pathway, as these proteins are involved in the storage of effectors within the bacterial cytoplasm, which allows the delivery of effectors to target cells immediately upon contact of the bacterium with the host cells. Most class IA chaperones are highly specialized and bind to only one effector, with the exception of CesT, which was recently reported to bind two effectors (Creasey *et al*, 2003). In contrast, the class IB chaperones Spa15 and InvB each associate with at least three effectors that do not exhibit detectable sequence similarity (Page *et al*, 2002; Ehrbar *et al*, 2003). Here, we provide a structural basis for the proposed classification of class I chaperones into two groups by showing that the structure of the Spa15 class IB chaperone is related to that of class IA chaperones but exhibits some notable differences as compared with these other chaperones. Both types of chaperones have the same general architecture of a β-sheet surrounded by three α-helices and have four hydrophobic patches on the surface of the chaperone dimer. A main difference, however, lies at the dimer interface. In Spa15, the α2 helices have a different orientation, leading to a dimer in which the subunits are rotated about 30° with respect to each other. The residues that are important for the different shape and orientation of the α2 helix are conserved among other putative class IB chaperones and are a means of distinguishing class IA and IB chaperones (Fig 1). The generally greater conservation of sequence and, most probably, structure of class IB chaperones might be linked to their broad

chaperoning activity, as multiple interacting effectors would impose more constraints on the chaperone structure.

The hydrophobic patches that are involved in the binding of the effector on class IA chaperones are present on the surface of Spa15, and also show a similar mix of conservation and deviation. The hydrophobic groove in Spa15 is very similar to class IA grooves, and although the residues in this groove are not conserved between class IA and IB chaperones, Trp 55 in Spa15 is present at the same position as Phe 49 of SycE, which is engaged in strong interactions with the effector helix. In contrast, the hydrophobic pocket is differently shaped. The extended α1 helix and the Pro-41-mediated altered β1–β2 loop conformation work together to change the exact location of the pocket, but the hydrophobic nature of the pocket is retained, including the presence of acidic residues that could possibly interact with a basic residue of an effector. Moreover, the stretch of residues that connects α1 and β1, which shows considerable variation and flexibility among all class I chaperones, is distinctly longer in Spa15 and its class IB homologues (Fig 1), and its conformation in the crystal structure prohibits any strand-pairing interactions in the groove near β1. The broad conservation of these different features in class IB chaperones suggests that a different pocket might be relevant for the function of class IB chaperones.

Similarly to class IA chaperones, it is likely that the Spa15 hydrophobic patches are involved in the binding of substrates. Yet, whereas the YopE(23–78) and SptP(36–139) polypeptides follow very similar paths around their respective chaperones (Birtalan *et al*, 2002), the specific Spa15 subunit orientation would dictate a different conformation for the Spa15 substrate polypeptides in their path around the Spa15 dimer. The most notable differences might be expected in the crossover from one chaperone subunit to the other, as the Spa15 surface landscape in this area is most dissimilar to class IA chaperones. The structure of Spa15 and its comparison with class IA chaperones clearly suggest how class IB chaperones might be able to bind to and stabilize their substrates. With its putative helix-binding site made up of the rigid β-sheet and its hydrophobic pocket sitting in between the β-sheet and two helices, the Spa15 dimer presents itself as a stable binding platform for its effectors. It is therefore likely that Spa15 effectors, despite their lack of detectable sequence similarity, share structural similarity and all possess two appropriately spaced helices to fill the Spa15 helix-binding sites and two hydrophobic patches to occupy the Spa15 hydrophobic pockets. Charge complementarity between the negatively charged Spa15 and the positively charged potential N-terminal chaperone-binding regions of IpgB1, IpaA, OspC and OspB might contribute to the strength of the Spa15 effector binding.

Chaperones not only bind to and stabilize their effectors in the bacterial cytoplasm, but also maintain them in a secretion-competent state. Indeed, upon activation of the TTSA, secretion of presynthesized YopE is dependent on SycE in *Yersinia* (Lloyd *et al*, 2001), whereas in *Shigella* presynthesized IpaA requires Spa15 for secretion (Page *et al*, 2002). In contrast, YopE and IpaA molecules that are produced while the TTSA is active do not require the chaperone to transit through the TTSA. Birtalan *et al* (2002) have proposed a model in which the structurally conserved chaperone–effector complex functions as a universal 3D secretion signal. However, structural differences between the Spa15 and SycE dimers should lead to a different 3D organization of the effector–chaperone complex, suggesting that the class I TTS chaperone family harbours more structural diversity than was previously anticipated. Such a structural diversity does not favour a model featuring conserved and specific interactions between the effector–chaperone complex and components of the TTSA. Alternatively, as the chaperone-binding region of the effector is located immediately downstream from the N-terminal secretion signal, the binding of class I chaperones to the effector might ensure that the secretion signal carried by the effector is exposed, or accessible, to be recognized by components of the TTSA (Parsot *et al*, 2003). In this model, the overall similarity of class I chaperones might still have a role in ensuring a proper orientation towards the TTSA.

METHODS

Overexpression and purification. Spa15 was expressed in *E. coli* DH5α as a recombinant protein with an N-terminal His_6 tag (Page *et al*, 2002). Cells were grown in Luria–Bertani medium at 298 K and expression was induced with isopropyl-β-D-thiogalactoside. Cells were resuspended in a buffer containing 20 mM Tris–HCl (pH 8), 1 M NaCl and 30 mM imidazole and sonicated, after which the soluble fraction was applied to a HiTrap Chelating HP column (Pharmacia), loaded with Co^{2+}. His-tagged Spa15 was eluted with a buffer containing 20 mM Tris–HCl (pH 8), 100 mM NaCl and 300 mM imidazole, dialysed against 20 mM Tris–HCl (pH 8), 25 mM NaCl and 1 mM dithiothreitol (DTT) and afterwards applied to a Source15Q anion exchange column and eluted by a linear gradient from 25 to 500 mM NaCl in a buffer also containing 20 mM Tris–HCl (pH 8) and 1 mM DTT. Fractions containing Spa15 were pooled and finally applied to a Superdex75 HR 10/30 column in a buffer containing 20 mM Tris–HCl (pH 8), 100 mM NaCl and 1 mM DTT. L-SeMet-containing Spa15 was expressed in the same strain in M9 minimal medium by repressing methionine biosynthesis as described (Doublié, 1997). Purification was the same as for nonsubstituted Spa15.

Crystallization and data collection. Crystals were grown at 291 K with the hanging-drop method. Drops were a mixture of 2 μl of a 3 mg/ml protein solution (20 mM Tris–HCl (pH 8), 25 mM NaCl, 5 mM DTT) and 2 μl reservoir solution (100 mM MES (pH 5.5), 50 mM $(NH_4)_2SO_4$, 5% (v/v) ethylene glycol, 100 mM guanidium chloride). As a cryoprotectant the mother liquor was used, supplemented with 5 mM DTT and an increased ethylene glycol concentration of 25% (v/v). A native data set to 1.8 Å resolution was collected on a $P2_1$ crystal at ID14-2 (ESRF, France). A Se-MAD data set to 2.5 Å resolution was collected on a $P2_12_12_1$ crystal with related dimensions at BM30 (ESRF, France). Data were processed with DENZO/SCALEPACK (Otwinowski & Minor, 1997) and programs from the CCP4 package (CCP4, 1994) (Table 1).

Structure determination. The structure was solved by Se-MAD. A total of 7 out of 12 possible Se sites in the dimer were located using S*n*B (Weeks & Miller, 1999) and refined in *SOLVE* (Terwilliger & Berendzen, 1999). Two additional well-defined Se atoms escaped attention, probably because of their close proximity of 5–6 Å to other Se positions. *RESOLVE* (Terwilliger, 2003) was used to improve initial phases and to do initial tracing. The final model was obtained by cycles of manual building in XFIT (McRee, 1999) and refinement in Refmac5 (Murshudov *et al*,

Table 1 | Data collection and refinement statistics

Data collection				
	Native		**MAD**	
Space group	$P2_1$		$P2_12_12_1$	
Unit cell (Å)	$a = 50.9$		$a = 51.1$	
	$b = 87.7$		$b = 58.5$	
	$c = 58.7$		$c = 87.7$	
(deg)	$\beta = 90.8$			
		Peak	**Inflection**	**Remote**
Resolution (Å)	30–1.82 (1.89–1.82)		30–2.54 (2.63–2.54)	
Mosaicity (deg)	0.46	0.83	0.88	0.98
Wavelength (Å)	0.9196	0.9794	0.9795	0.9760
Completeness (%)	97.4 (92.3)	99.4 (95.6)	99.2 (93.8)	98.6 (91.5)
Redundancy	4.8	12.6	11.8	5.1
Unique reflections	45,246	9,026	9,057	9,044
$I/\sigma(I)$	15.7 (2.5)	18.3 (10.4)	26.1 (10.7)	16.8 (5.3)
R_{sym} [a] (%)	5.5 (39.3)	11.7 (18.1)	8.4 (16.7)	7.6 (20.5)
Phasing				
Figure of merit	After *SOLVE*		0.54	
	After *RESOLVE*		0.64	
Refinement				
R/R_{free} [b] (%)	18.1/21.1			
Avg. *B* factor (Å^2)	24.7			
R.m.s.d.				
Bonds (Å)	0.006			
Angles (deg)	1.2			

Values in parentheses are for the highest resolution shell.
[a] $R_{sym} = \sum|I - \langle I\rangle|/\sum I$, where I is the observed intensity and $\langle I\rangle$ the average intensity.
[b] $R = \sum_{hkl,\ work}||F_{obs}| - k|F_{calc}||/\sum_{hkl}|F_{obs}| \times 100\%$, where F_{obs} is the observed structure factor and F_{calc} is the calculated structure factor. R_{free} is R calculated with 5% of the randomly selected data that were omitted from the refinement.

1999). The coordinates and structure factors have been deposited in the PDB (accession code 1RY9).

SAXS. Experiments were performed on the small-angle instrument D24 at LURE (Orsay, France). Samples were contained in an evacuated cell (Dubuisson *et al*, 1997) at 9°C. The sample-to-detector distance was 1,133 mm and the X-ray wavelength was 1.488 Å. Eight frames of 200 s were recorded for each sample. The intensity curves were scaled to the transmitted beam intensity before background subtraction. The final Spa15 scattering curve was obtained after merging the high-angle region of the curve obtained from a 7.6 mg/ml Spa15 solution (also containing 20 mM Tris–HCl (pH 8), 100 mM NaCl and 10 mM DTT) and the low-angle region of the curve obtained from a diluted Spa15 solution (3.8 mg/ml, after gel filtration) for which no significant interactions could be detected at very low angles. The program CRYSOL (Svergun *et al*, 1995) was used to calculate the scattering curves from the crystallographic coordinates of Spa15.

ACKNOWLEDGEMENTS

This research was supported in part by The Netherlands Foundation of Chemical Research (CW), with financial aid from The Netherlands Foundation for Scientific Research (NWO). C. Hamiaux was supported by a European Community Marie Curie fellowship.

REFERENCES

Birtalan S, Ghosh P (2001) Structure of the *Yersinia* type III secretory system chaperone SycE. *Nat Struct Biol* **8:** 974–978

Birtalan SC, Phillips RM, Ghosh P (2002) Three-dimensional secretion signals in chaperone–effector complexes of bacterial pathogens. *Mol Cell* **9:** 971–980

Collaborative Computational Project, Number 4 (1994) The CCP4 suite: programs for protein crystallography. *Acta Crystallogr D* **50:** 760–763

Cornelis GR (2003) How Yops find their way out of *Yersinia*. *Mol Microbiol* **50:** 1091–1094

Creasey EA *et al* (2003) CesT is a bivalent enteropathogenic *Escherichia coli* chaperone required for translocation of both Tir and Map. *Mol Microbiol* **47:** 209–221

Doublié S (1997) Preparation of selenomethionyl proteins for phase determination. *Methods Enzymol* **276:** 523–530

Dubuisson JM, Decamps T, Vachette P (1997) Improved signal-to-background ratio in small-angle X-ray scattering experiments with synchrotron radiation using an evacuated cell for solutions. *J Appl Crystallogr* **30:** 49–54

Ehrbar K, Friebel A, Miller SI, Hardt WD (2003) Role of the *Salmonella* Pathogenicity Island 1 (SPI-1) protein InvB in type III secretion of SopE and SopE2, two *Salmonella* effector proteins encoded outside of SPI-1. *J Bacteriol* **185:** 6950–6967

Evdokimov AG, Tropea JE, Routzahn KM, Waugh DS (2002) Three-dimensional structure of the type III secretion chaperone SycE from *Yersinia pestis*. *Acta Crystallogr D* **58:** 398–406

Hueck CJ. (1998) Type III protein secretion systems in bacterial pathogens of animals and plants. *Microbiol Mol Biol Rev* **62:** 379–433

Lloyd SA, Norman M, Rosqvist R, Wolf-Watz H (2001) *Yersinia* YopE is targeted for type III secretion by N-terminal, not mRNA, signals. *Mol Microbiol* **39:** 520–531

Luo Y *et al* (2001) Structural and biochemical characterization of the type III secretion chaperones CesT and SigE. *Nat Struct Biol* **8:** 1031–1036

McRee DE (1999) XtalView/Xfit—a versatile program for manipulating atomic coordinates and electron density. *J Struct Biol* **125:** 156–165

Murshudov GN, Vagin AA, Lebedev A, Wilson KS, Dodson EJ (1999) Efficient anisotropic refinement of macromolecular structures using FFT. *Acta Crystallogr D* **55:** 247–255

Otwinowski Z, Minor W (1997) Processing of X-ray diffraction data collected in oscillation mode. *Methods Enzymol* **276:** 307–326

Page AL, Parsot C (2002) Chaperones of the type III secretion pathway: jacks of all trades. *Mol Microbiol* **46:** 1–11

Page AL, Fromont-Racine M, Sansonetti P, Legrain P, Parsot C (2001) Characterization of the interaction partners of secreted proteins and chaperones of *Shigella flexneri*. *Mol Microbiol* **42:** 1133–1145

Page AL, Sansonetti P, Parsot C (2002) Spa15 of *Shigella flexneri*, a third type of chaperone in the type III secretion pathway. *Mol Microbiol* **43:** 1533–1542

Parsot C, Hamiaux C, Page AL (2003) The various and varying roles of specific chaperones in type III secretion systems. *Curr Opin Microbiol* **6:** 7–14

Ramamurthi KS, Schneewind O (2003) Substrate recognition by the *Yersinia* type III protein secretion machinery. *Mol Microbiol* **50:** 1095–1102

Stebbins CE, Galán JE (2001) Maintenance of an unfolded polypeptide by a cognate chaperone in bacterial type III secretion. *Nature* **414:** 77–81

Svergun D, Barberato C, Koch MHJ (1995) CRYSOL—a program to evaluate X-ray solution scattering of biological macromolecules from atomic coordinates. *J Appl Crystallogr* **28:** 768–773

Terwilliger TC (2003) Automated main-chain model building by template matching and iterative fragment extension. *Acta Crystallogr D* **59:** 38–44

Terwilliger TC, Berendzen J (1999) Automated MAD and MIR structure solution. *Acta Crystallogr D* **55:** 849–861

Weeks CM, Miller R (1999) The design and implementation of S*n*B version 2.0. *J Appl Crystallogr* **32:** 120–124